Acta Cryst. (1993). A**49**, 881–889

Properties of Molecular Crystals by Means of Theory

BY ITAI PANAS

Department of Inorganic Chemistry, University of Göteborg and Chalmers University of Technology, S-412 96 Göteborg, Sweden

(*Received* 25 *November* 1992; *accepted* 19 *May* 1993)

Abstract

A novel quantum-chemical approach to the properties of molecular crystals has recently been developed. This Hartree–Fock-based self-consistent-crystal-field method is outlined and applied to the intramolecular torsion angle in solid hydrogen peroxide, the cold-phase structure of solid dinitrogen and the hot-phase structure of solid acetylene. The potential-energy surfaces are calculated with the assumption of perfectly ordered crystals and coherent molecular potential-energy surfaces are produced. Agreement with experiment is obtained for hydrogen peroxide. It is suggested that discrepancies between calculated and observed structures of $N_2(s)$ and $C_2H_2(s)$ result from static and dynamic disorder, respectively. This interpretation is consistent with the experimentally observed intramolecular-bond shortenings in these two solids. Lattice energies in good agreement with experiment are obtained in all three cases.

1. Introduction

The structures and physical properties of molecular crystals are generally understood in terms of the properties of the molecular constituents, their intermolecular electrostatic and van der Waals interactions, charge penetrations and Pauli repulsion. The challenge for a theoretical chemist in this field is in formulating a quantitative method to calculate the interactions in a molecular crystal, which profits from these concepts.

Two approaches have been assumed previously and these are referred to as methods (*a*) and (*b*) below. In method (*a*), accurate pair potentials are produced for the dimer from *ab inito* quantum-chemical calculations and these pair potentials are subsequently employed to obtain the properties of the solid. Excellent results for the properties of solid nitrogen have been obtained by Berns & van der Avoird (1980) and van der Avoird, Wormer & Jansen (1986) employing method (*a*), the drawbacks being that the dispersion of the electronic bands cannot be produced and that only two-body interactions are included in that approach. Method (*b*) is represented by the program package *CRYSTAL* (Dovesi, Saunders & Roetti, 1992), which solves the Roothan–Hartree–Fock equations for an infinite crystal. This second approach has produced excellent results for ionic solids, both with regard to electronic-band structures and crystal structures, although superposition errors and the absence of a dispersion-interaction description have effectively prevented it from addressing the structural properties of molecular solids.

The purpose of the present work is to present a novel quantum-chemical approach to the properties of molecular solids. The Hartree–Fock-based self-consistent crystal field (HF-SCCF) method can be viewed as a synthesis of methods (*a*) and (*b*). It is outlined in § 2. Similar to method (*a*), HF-SCCF assumes negligible dispersion of electronic bands but, while method (*a*) parametrizes the intermolecular pair interaction in a separate set of calculations on the dimer, the HF-SCCF approach is integrated into the *ab initio* quantum-chemical program package. Hence, the molecular HF-SCCF wave function is optimized in the crystal environment in the same sense as in method (*b*). The advantages of the HF-SCCF approach compared with method (*b*) are (i) dispersion interaction and intramolecular electron correlation can be formulated, thanks to the localized description, and (ii) superposition errors do not appear.

The drawback of the HF-SCCF approach compared to method (*b*) is that a parameter needs to be introduced to scale the Pauli repulsion expression (see § 2) and that the dispersion of electronic bands is neglected as in method (*a*). Hence, only *CRYSTALS* is truly *ab initio*.

The HF-SCCF method is presented in § 2 and some applications are presented in § 3.

2. Method

The development of the Hartree–Fock-based self-consistent crystal field (HF-SCCF) method was presented by Panas (1992, 1993*a*,*b*) where it is applied to solid HCN and to the FCN dimer. HF-SCCF employs the well known bipolar expansion expres-

ISSN 0108-7673

sion (see *e.g.* Hirschfelder, Curtiss & Bird, 1954)

$$r_{12}^{-1} = \sum_{l_A m_A} M_{l_A}^{m_A}(\mathbf{r}_1 - \mathbf{r}_A) \times \sum_{l_B m_B} I_{l_A+l_B}^{-m_A-m_B}(\mathbf{r}_A - \mathbf{r}_B) M_{l_B}^{m_B}(\mathbf{r}_B - \mathbf{r}_2) \quad (1)$$

to calculate the lattice energy of a molecular crystal as a function of the crystal structure. $M_l^m(\mathbf{r} - \mathbf{r}_A)$ and $I_l^m(\mathbf{r}_A - \mathbf{r}_B)$ are the regular and irregular solid harmonics and $\mathbf{r}_A$ and $\mathbf{r}_B$ are the origins of the two charge distributions. Crucial for this approach is that the crystal wave function can be approximately factorized into a product of molecular wave functions. In the case of a single symmetry-independent molecule, the HF-SCCF scheme becomes particularly transparent, as the following outline indicates.

(i) The wave function of the explicitly described molecule is multipole expanded to high orders ($l_{\max} = 18$).

(ii) The multipole-expanded charge distribution is placed at the lattice points given by the proposed crystal structure.

(iii) An Ewald summation technique is employed (Panas, 1992) to account for the dipole contributions to the dipole field.

(iv) The contributions to the dipole field ($l = 1$) from higher multipoles and the multipole field contributions for $l > 1$ are converged in direct space by calculating these contributions at the centre of a $20 \times 20 \times 20$ unit-cell slab.

(v) A first-order renormalization correction to the Coulombic multipole field is introduced to account for the Pauli repulsion with the nearest neighbours according to

$$\Delta E_{l_A}^{m_A} = k S_{\text{ave}}^{AB} \sum_{l_B m_B} I_{l_A+l_B}^{-m_A-m_B}(\mathbf{r}_A - \mathbf{r}_B) \times [\mathsf{M}_{l_B}^{m_B}(\text{nuc.}) - (1/2)\mathsf{M}_{l_B}^{m_B}(\text{el.})] \quad (2)$$

where summation over m_B and l_B is implicit, k is a parameter to be fitted to experimental (Panas, 1993*a*) or *ab initio* (Panas, 1993*b*,*c*) results; M_l^m(nuc.) and M_l^m(el.) are the multipole-expanded nuclear and electronic charge distributions, respectively, and

$$S_{\text{ave}}^{AB} = [1/(N_{\text{el}}^A)^2] \sum_{i \in A} \sum_{k \in B} \langle i|k\rangle\langle k|i\rangle. \quad (3)$$

The summations in (3) are over occupied orbitals.

(vi) A Hartree–Fock iteration is performed with the intermolecular Fock matrix contribution

$$F_{\mu\nu}^A(\text{inter.}) = \sum_{l_A m_A} (\mu|M_{l_A}^{m_A}|\nu) E_{l_A}^{m_A}, \quad (4)$$

where

$$E_{l_A}^{m_A} = \sum_{B \neq A} \sum_{l_B m_B} I_{l_A+l_B}^{-m_A-m_B}(\mathbf{r}_A - \mathbf{r}_B)\mathsf{M}_{l_B}^{m_B}(\text{el.} + \text{nuc.}). \quad (5)$$

$E_{l_A}^{m_A}$ is the effective multipole field experienced by the monomer A from all other monomers B, $\mathsf{M}_{l_B}^{m_B}$ (el. + nuc.) is the multipole expansion of the charge distribution of monomer B.

(vii) (i)–(vi) are repeated until convergence is reached.

(viii) The dispersion interaction with a $6 \times 6 \times 6$ unit-cell environment is obtained by adding the Coulombic pair interaction contributions in second-order Møller–Plesset perturbation theory (MP2):

$$E_{\text{disp}} = 4(1/2) \sum_{i \in A} \sum_{a \in A} \sum_{j \in B} \sum_{b \in B} (1 - P) \times [|\langle ij|\mathbf{r}_{12}^{-1}|ab\rangle|^2/(\varepsilon_i + \varepsilon_j - \varepsilon_a - \varepsilon_b)], \quad (6)$$

where $P = k[\langle i|b\rangle\langle b|i\rangle + \langle j|a\rangle\langle a|j\rangle]$. A and B are the interacting monomers. If intermolecular orbital and charge overlaps can be neglected ($P = 0$), the molecular orbital integrals in (6) can be written in the bipolar expansion language

$$\langle ij|\mathbf{r}_{12}^{-1}|ab\rangle = M_{l_{A,ia}}^{m_{A,ia}} I_{l_A+l_B}^{-m_A-m_B}(\mathbf{r}_A - \mathbf{r}_B) M_{l_{B,jb}}^{m_{B,jb}}, \quad (7)$$

where $M_{l_{A,ia}}^{m_{A,ia}}$ and $M_{l_{B,jb}}^{m_{B,jb}}$ are the multipole expansions of the molecular orbital pairs $\phi_i\phi_a$ and $\phi_j\phi_b$, respectively. Summations over the indices m_a, m_b, l_a and l_b are assumed implicitly. The expression P is a correction to the dispersion interaction in the limit of small intermolecular overlaps;

(ix) The intramolecular electron correlation is added by means of MP2 (applied in the investigation of the α phase of solid dinitrogen).

The intramolecular interactions are calculated in a conventional way by employing the *ab initio* quantum-chemical program package *DISCO* written by Almlöf, Faegri, Feyereisen & Korsell (1991).

3. Applications

The examples below have been chosen to demonstrate what information of crystallographic relevance can be expected from the HF-SCCF approach. The emphasis in this presentation is upon the qualitative features of the results produced. Thus, only potential-energy curves resulting from retricted geometry changes have been calculated. Standard basis sets of 6-31G** including one extra function of *s* and *p* type have been employed [see *e.g.* Hinchliffe, 1987 and references therein) for definition].

In § 3*A*, the intramolecular torsion angle in solid hydrogen peroxide is investigated and results in excellent agreement with experiment are obtained. In § 3*B*, the cold-phase structure of solid dinitrogen and the hot-phase structure of solid acetylene are dealt with. In the latter two cases, the interpretations are more complicated and disorder in the solids [static in $N_2(s)$ and dynamic in $C_2H_2(s)$] is proposed.

A. Solid hydrogen peroxide

The torsion angle of free H_2O_2 has only recently been established. Two values, 111.5 and 119.1°, have been advocated and convincing arguments in favour of the former presented by Koput (1986).

In contrast to the understanding of the free molecule, the molecular structure in $H_2O_2(s)$ has been known for quite some time. The tetragonal space group of the solid, $P4_12_12_1$ with $a = 4.06$ (2) and $c = 8.00$ (2) Å, and the positions of the O atoms were determined by Abrahams, Collin & Lipscomb (1951) in an early X-ray study. The issue of the positions of the H atoms was settled by Busing & Levy (1958, 1959) by neutron diffraction. They later published a detailed analysis of their results (Busing & Levy, 1965). The intramolecular parameters are $R_{O-O} = 1.453$ (7), $R_{O-H} = 0.988$ (5) Å, O–O–H = 102.7 (3)° and the torsion angle between the H(1)–O(1)–O(2) and O(1)–O(2)–H(2) planes is 90.2 (6)°. The structure is uniquely determined by the parameters [$O_x = 0.0731$ (4), $O_y = 0.1670$ (4), $O_z = 0.2213$ (2)] and [$H_x = -0.0473$ (11), $H_y = 0.2838$ (9), $H_z = 0.1317$ (4)].

In the present study, the scaling factor $k = 1.12$ (§ 2) was determined by requiring the lattice constant a to have the observed value, while c was found to be 7.9 Å, in reasonable agreement with experiment.

Subsequently, the torsion angle was investigated while unit-cell dimensions, intramolecular bond distances, O–O–H angles and O-atom positions were taken to be the experimental values in the solid. Hence, the torsion angle was the only intramolecular degree of freedom to be optimized both for the free molecule and for the molecules in the solid. In the case of the former, 114.5° was obtained by the Hartree–Fock theory.

The potential-energy curve and its decomposition into dispersive and nondispersive contributions are displayed in Fig. 1. These curves correspond to all the molecules in the solid undergoing the same change in torsion angle. The optimal angles for the dispersive and nondispersive contributions are 101.5 and 83.0°, respectively. The resulting value, 90.4°, for the effective potential-energy curve is obviously in excellent agreement with experiment. While it is hard to asses to what quantitative degree this result is fortuitous, the overall picture of the two contributions with optimal angles displaced by about 10° to larger and smaller values relative to the experimental result is unambiguous.

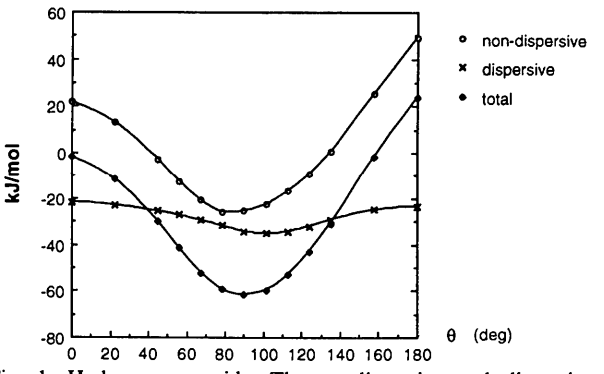

Fig. 1. Hydrogen peroxide. The nondispersive and dispersive contributions and the total binding energy are displayed as functions of the torsion angle and the optimal angles are 83.0, 101.5 and 90.4°, respectively. 0 and 180° correspond to *cis* and *trans* arrangements of the H atoms in the molecule, respectively. The experimental value is 90.2 (6)°.

A 60.5 kJ mol^{-1} lattice-energy estimate is obtained by subtracting the energy for the optimal torsion angle in the free molecule from that in the solid. This value is in qualitative agreement with the experimentally estimated 65.5 kJ mol^{-1} heat of sublimation by Giguère, Morissette & Olmos (1954) [quoted by Guigère & Secco (1954)].

B. Disorder in molecular crystals

Disorder in a crystal is generally divided into two categories, static and dynamical. The dynamical disorder is generally perceived in terms of isotropic and anisotropic vibrational thermal motion relative to a structure belonging to a specific space group. An additional aspect of this subject was provided by Pauling (1930) who proposed that the incoherent motion in a molecular crystal is vibrational and rotational in the two limiting cases of strong and weak crystal fields. Several molecular crystals are suggested to undergo succesive phase transitions upon cooling, corresponding to increasingly hindered rotational motion. Below, the cold-phase structure of solid nitrogen and the hot-phase structure of solid acetylene are addressed. Results suggestive of static and dynamical (molecular precession) disorder for the two solids are obtained.

The present approach assumes ordered crystal structures, subjected to restricted coherent optimizations of the molecular orientations. Obviously, such coherent-potential-energy curves are not true images of a real crystal. Hence, the results produced below must necessarily be of a suggestive and qualitative nature.

(i) *α-Nitrogen.* Solid nitrogen has one high-temperature phase, the β phase, and one low-temperature phase, the α phase. In the case of the β phase, X-ray diffraction data alone (Jordan, Smith, Streib & Lipscomb, 1964; Streib, Jordan & Lipscomb 1962) were consistent with both statically and dynamically disordered molecular orientations. A preference for a description where the molecules precess with 56° conic angles was indicated. This preference was based on an anomaly in the specific-heat measurement by Giauque & Clayton (1933) in the temperature region of the transition.

Two crystal structures have been proposed for α-N_2, corresponding to the space groups $Pa3$ and $P2_13$ (see Fig. 2). $P2_13$ was initially proposed by Vegard (1929), who determined a cubic unit cell with $a = 5.67$ Å and $R_{N-N} = 1.07$ Å at 20 K. This bond distance is in reasonable agreement with the gas-phase value 1.0975 (1) Å (*Handbook of Chemistry and Physics*, 1988–89). Later, Ruhemann (1932) and Bolz, Boyd, Mauer & Peiser (1959) proposed the space group $Pa3$ to be the correct choice owing to the absence of the 110 and 310 reflections. They obtained $a = 5.68$ and $a = 5.662$ Å, respectively. The former value was measured at 20 K, while the latter is an extrapolation from a 13 K measurement. Ruhemann does not report an intramolecular bond distance while Bolz *et al.* give $R_{N-N} = 1.056$ Å. Bolz *et al.* were not fully convinced of the space group $Pa3$ though, probably due to the presence of structural faults. Support for a perturbed structure is provided from thin-film electron diffraction measurements by Höhrl & Marton (1961), who were able to determine a unit cell with $a = 5.661$ Å, assuming the $Pa3$ space group. Based on the electron diffraction data, Donohue (1961) refined the structure with respect to the positional parameter and obtained $R_{N-N} = 1.04$ (4) Å. The possibility of α-N_2 having the space group $P2_13$ was again suggested by Jordan, Smith, Streib & Lipscomb (1964) on the basis of faint reflections incompatible with $Pa3$. These authors obtained a much better agreement between the gas-phase bond distance and that in the solid by assuming a polar structure. Later though, in another X-ray study, Schuch & Mills (1970) could not confirm the presence of these reflections.

The structure of α-N_2 has also been addressed by means of infrared and Raman spectroscopy (St. Louis & Schnepp, 1969; Brith, Ron & Schenpp, 1969; Cahill & Leroi, 1969; Anderson, Sun & Dunkersloot, 1970). No evidence for a noncentrosymmetric space group was found. One IR study by Wachtel (1972) is in favour of $P2_13$. Arguments against a $P2_13$ space group have also been raised from the electron diffraction measurements by Venables (1970) and Venables & English (1974). The latter authors proposed the reflections associated with the $P2_13$ space group to result from structural faults or possibly twinning. Evidence of piezoelectricity implying a noncentrosymmetric space group, produced by Brookeman & Scott (1972) as well as the IR measurement by Wachtel (1972) were both explained by documented strains in α-N_2 (Gannon & Morrison, 1973). Hence, that α phase is reported to shatter unless annealed close to the transition temperature for about 12 h.

A conclusion that can be drawn from the experimental results is that α-N_2 crystallizes either in ordered $P2_13$ or in disordered $Pa3$. Fig. 3(*a*) displays the calculated potential energy as a function of the

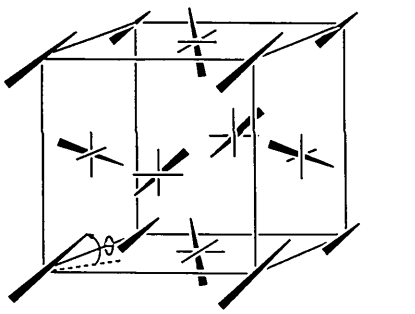

Fig. 2. A cubic unit cell under consideration. The molecules are depicted as bars. The space group is $Pa3$ if $\theta = 35.264°$ and the bars intersect the unit cell at their midpoints. The space group is $P2_13$ if $\theta = 35.264°$ and the bars intersect the unit cell asymmetrically.

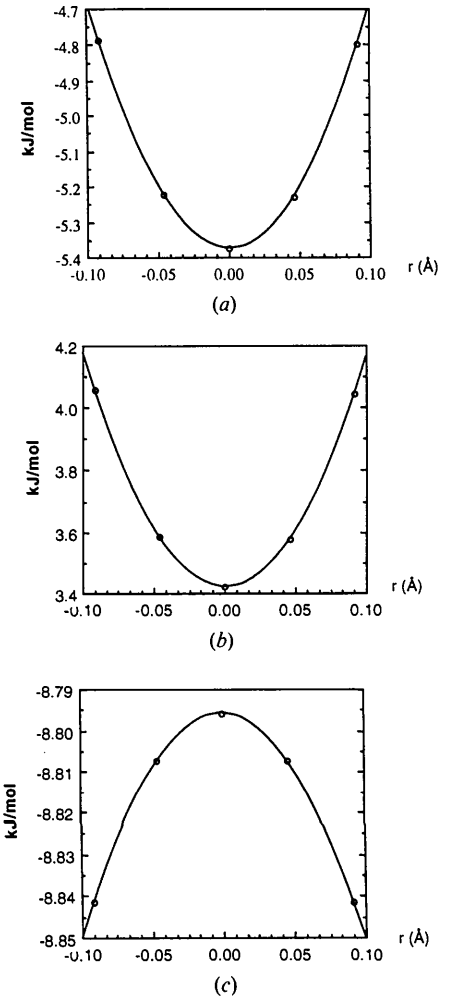

Fig. 3. Dinitrogen. The potential-energy curve (*a*) is obtained by displacing the molecules from the space diagonals. $r \neq 0$ corresponds to the $P2_13$ space group, while $r = 0$ corresponds to the $Pa3$ space group. (*b*) and (*c*) are the nondispersive and dispersive contributions, respectively.

displacement **r** along the ⟨111⟩ direction. This result evidently favours the *Pa*3 space group. In this investigation, the scaling factor $k = 0.72$ (§ 2) was determined by requiring the lattice constant a of the cubic unit cell to have the measured value for the *Pa*3 structure. The decomposition of the net potential energy into nondispersive and dispersive contributions (Figs. 3*b* and 3*c*) reveals a slightly more complicated picture. While the nondispersive contribution favours the *Pa*3 structure, the dispersive one is maximally unfavourable at this point. Still, it is felt that the *Pa*3 space group is preferable because, apart from the fact that the net contribution is in favour of this space group, the introduction of thermal motion into the description would enhance this result. This is gratifying, since the *Pa*3 space group is consistent with most experimental findings of a nonpolar unit cell.

So, the apparent shortening in the intramolecular bond distance in α-N_2 is proposed to result from disorder. In order to investiage this hypothesis, the section of the coherent-potential-energy surface in the plane spanned by the ⟨001⟩ and ⟨110⟩ directional vectors (Fig. 2) was calculated. The coherent-potential-energy curve was calculated in the *Pbca* space group, for which a particular orientation corresponds to *Pa*3, and is displayed in Fig. 4(*a*). Note the shallow potential-energy curve and the fact that the global minimum is in the ⟨001⟩ direction (at 90°) rather than in the ⟨111⟩ direction (at 35.264°) as would be expected for the *Pa*3 structure. A decomposition of the net potential-energy curve into nondispersive and dispersive contributions (Figs. 4*b* and *c*) reveals two antagonistic features. Hence, there is a competition between the repulsive nondispersive contribution, which has its minimum in the ⟨111⟩ direction, and the dispersive contribution, which has its global optimum in the ⟨001⟩ direction. The fact that the nondispersive contribution is shallower than the dispersive contribution determines the shape of the net potential-energy curve. The lattice energy obtained, 5.4–5.9 kJ mol^{-1}, is in qualitative agreement with the estimated 6.9 kJ mol^{-1} heat of sublimation of Kelley (1935).

The qualitative feature of the competition between two antagonistic contributions is evident from Fig. 4. The interpretation is straightforward, in that the molecules avoid each other optimally in a *Pa*3 arrangement and so the Pauli repulsion has a minimum for $\theta = 35.3°$. The price to be paid is that the distance between the molecular charge distributions is maximized, which in turn minimizes the attractive dispersion interaction.

The double-minimum property of the coherent-potential-energy surface is apparently at odds with the results of van der Avoird *et al.* (1986). One source of this discrepancy, assuming that these authors have investigated the coherent-potential-energy surface for molecular orientations at sufficiently large angular deviations from the space diagonals, could be that parametrization to mimic the coupling between intermolecular and intramolecular electron correlation was introduced in that work. In order to estimate the effect such a correction might have on the overall potential-energy surface, intramolecular electron correlation was introduced *via* second-order Møller–Plesset perturbation theory (see *e.g.* Szabo & Ostlund, 1982). The result is displayed in Fig. 5. While the overall characteristics of the potential-energy-surface remain, the energy difference between the molecular arrangements along the space diagonals and axes of the unit cell is reduced by some 60%. Hence, the stability ordering of the two minima might be artificial, while a stable axial arrangement cannot be excluded. The improved

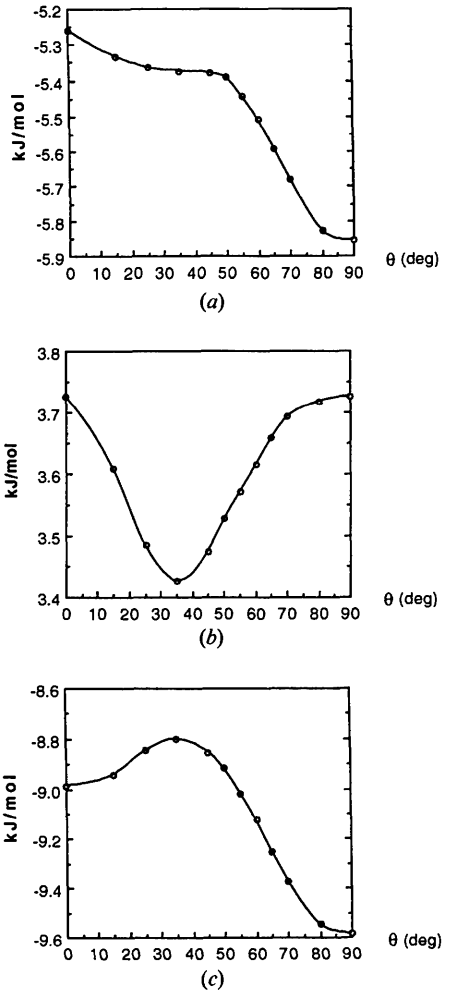

Fig. 4. Dinitrogen. The net potential-energy curve (*a*) is displayed, together with the (*b*) nondispersive and (*c*) dispersive contributions to the lattice energy as functions of the angle θ (see Fig. 2).

agreement with the experimentally obtained lattice energy is probably fortuitous, however, because changes in zero-point vibrations, for example, have not been taken into account.

There is some experimental evidence of disorder in the α phase of solid dinitrogen. Hence, a scenario of two counteracting lattice-energy contributions, causing instabilities in the solid, does not contradict experiment. Also the observed 4–6% bond shortening, compared with the gas phase, can be understood in terms of a static distribution of molecules aligned along the unit-cell axes and in the $\langle 111 \rangle$ direction. The sparseness of molecules along the axes explains why these have not been observed by Raman spectroscopy. Any asymmetry in the axial distribution could be an additional cause for an average polar unit cell, which has been observed by some experimentalists.

(ii) *Acetylene.* Indications for a precessional disorder in the hot-phase structure, similar to those suggested for β-N_2, can be found in solid acetylene. The two solid phases of acetylene have recently been subjected to accurate single-crystal neutron-diffraction measurements by McMullan, Kvick & Popelier (1992). Their results are in overall agreement with previous structure determinations based on neutron powder diffraction and single-crystal X-ray diffraction measurements, although they are generally of better quality [for references see McMullan *et al.* (1992)]. They found the hot-phase structure to be cubic with space group *Pa*3 (see Fig. 2), whereas the cold phase is orthorhombic with space group *Acam*. Characteristic of the hot-phase structure is a substantial shortening of the C–C bond distance, 1.138 Å, compared with the gas-phase value, 1.203 Å, measured by Fast & Wells (1972). As for the cold-phase structure at 15 K, the internuclear distance obtained is 1.193 Å, in much better agreement with the gas-phase value. The thermal-motion parameters for the cubic structure, deemed to be unusually large, were attributed mainly to rigid-body libration motion about the molecular centres of mass. Results for a structural description consistent with a molecular precession motion are presented below.

Similar to what was done for α-N_2, the scaling factor $k = 0.72$ (§ 2) was determined by requiring the lattice constant a of the cubic unit cell to have the experimentally determined value for the *Pa*3 structure. Two different sections through the coherent-potential-energy surface were considered. A *vertical* section was computed as depicted in Fig. 6(*a*) and the results are displayed in Fig. 7. Note the similar dispersive potential-energy curves in the present case and for α-N_2 (Figs. 4*c* and 7*c*). A *lateral* section through the potential-energy surface (Fig. 6*b* and Fig. 8) was also computed. This section corresponds to varying the direction of the molecular axis, parallel to one side of a tetrahedron, over an angle $0 \le \varphi \le 60°$. The tetrahedron is given by the midpoints of three adjacent surfaces and the corresponding corner of the unit cell (again, see Fig. 6*b*). All calculations were performed in the *Pbca* space group, as in the case of α-N_2.

A threefold degenerate global minimum emerges from Figs. 7(*a*) and 8, corresponding to the molecular orientations along the $\langle 110 \rangle$, $\langle 101 \rangle$ and $\langle 011 \rangle$ directions, as do also three equivalent saddle points at each of the three tetrahedral surfaces at directions corresponding to $\varphi = 30°$, $\theta = 50$–$55°$. A reason for

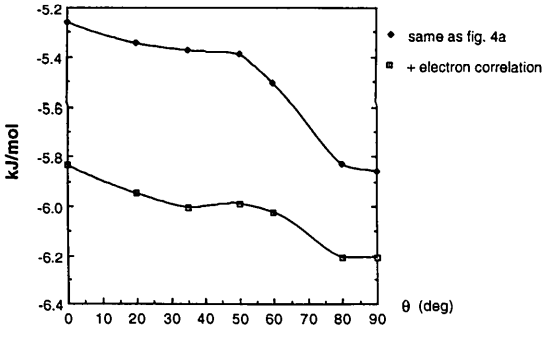

Fig. 5. Dinitrogen. The net potential-energy curve from Fig. 4(*a*) is compared with that including intramolecular correlation *via* MP2.

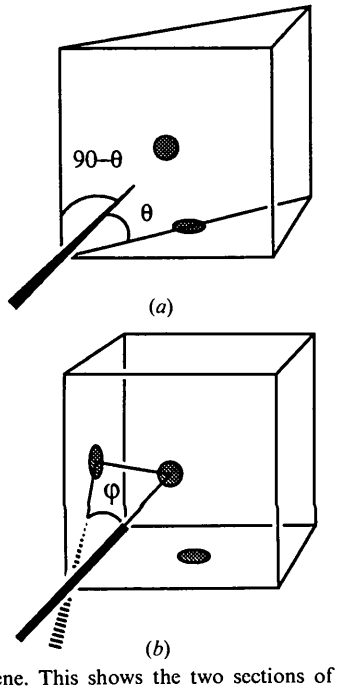

Fig. 6. Acetylene. This shows the two sections of the potential-energy surface for which calculations have been made. (*a*) The vertical section spanned by the directional vectors $\langle 001 \rangle$ and $\langle 110 \rangle$, $0 \le \theta \le 90°$ (as indicated in Fig. 2). (*b*) The lateral section. The arc indicates the motion of the molecule in the plane given by the surface of a tetrahedron ($0 \le \varphi \le 60°$).

the in-plane arrangements being attractive is the favourable electrostatic interaction between two quadrupoles in a 'head-to-waist' arrangement. A schematic potential energy surface is shown in Fig. 9.

The interpretation of the observed crystal structure in conjunction with the above calculations is straightforward, in that the molecules are proposed to precess around the space diagonals, the average structure corresponding to the *Pa*3 space group. The choice of description of the motion as precessional is based on the following:

(*a*) for high vibrational quantum numbers, the quantum-mechanical harmonic oscillator behaves like a classical oscillator;

(*b*) the global minima are the classically least probable positions while the positions most likely to be observed are the saddle points and at the classical turning points;

(*c*) the classical turning points would produce much shorter bond lengths than are observed;

(*d*) a precession motion with a 19° conic angle about the space diagonals would explain the apparent contraction of the molecule;

(*e*) an angle of ~15° from the ⟨111⟩ direction is obtained for the saddle points on the calculated static potential-energy surface.

Particularly notable is that a precessional motion can be viewed as resulting from two mutually perpendicular librational motions and, hence, the interpretation of McMullan *et al.* (1992) and that produced in the present study are complementary.

It is gratifying to note that any correction for the centrifiugal effect will move the saddle points towards the experimentally expected 19°. Such an effect is consistent with the observed temperature dependence in the lattice constant of the cubic unit cell, as discussed by McMullan *et al.* (1992)

The phase transition is suggested to progress through an initial slowing down of a precessional motion upon cooling, followed by the molecules being trapped at the surfaces of the unit cell to form parallel planar molecular sheets. This anisotropy in

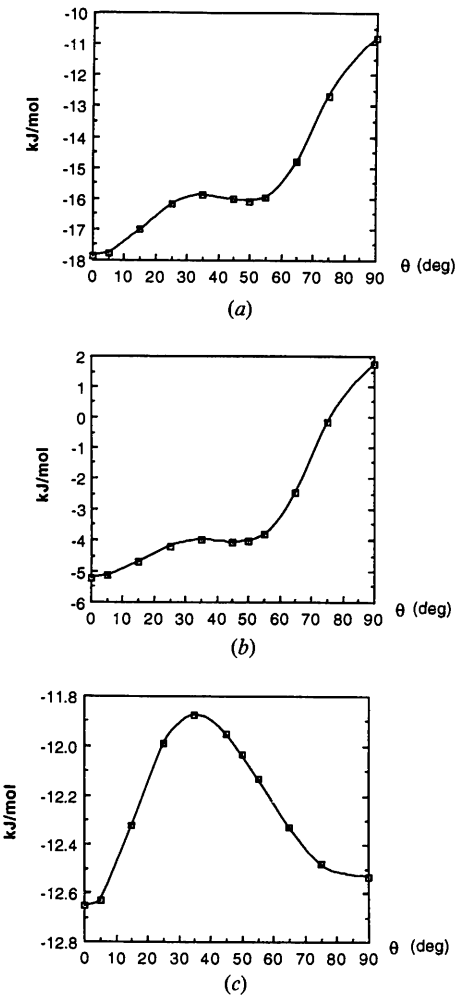

Fig. 7. Acetylene. The net potential-energy curve (*a*) is displayed together with the (*b*) nondispersive and (*c*) dispersive contributions to the lattice energy as functions of the angle θ (see Fig. 6*a*).

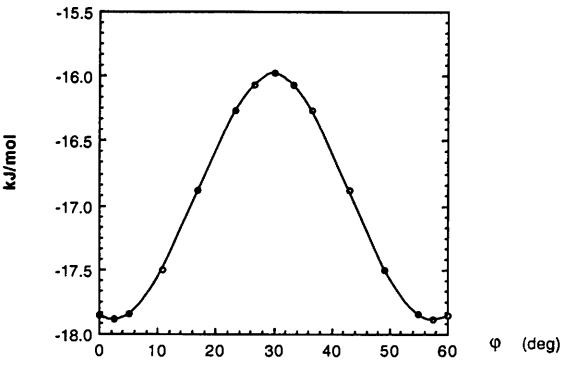

Fig. 8. Acetylene. The potential-energy curve corresponding to the section described in Fig. 6(*b*).

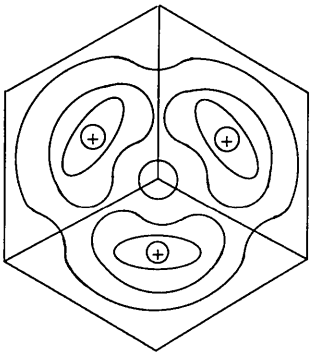

Fig. 9. Acetylene. A schematic description of the potential-energy surface. The + indicate the three degenerate minima and correspond to the molecules oriented along the three surfaces of the cube.

turn results in the transition from a cubic to an orthorhombic space group.

The above argument and scenario hold if (i) the molecular motion in the real solid is coherent at temperatures close to T_{trans} and (ii) *Pbca* symmetry is kept. Hence, the detailed agreement with experiment obtained, although appealing, might be fortuitous.

The obtained 16–18 kJ mol^{-1} lattice energy compares favourably with the 21.3 kJ mol^{-1} heat of sublimation, measured by Ambrose & Townsend (1964).

4. Concluding remarks

A novel Hartree–Fock-based self-consistent crystal field (HF-SCCF) method has been outlined in which dispersion interactions and intramolecular electron correlations are included at the second-order Møller–Plesset perturbation theory level. The HF-SCCF approach is an attempt to benefit from the common qualitative understanding of intermolecular and intramolecular interations to formulate an efficient and quantitative description of these interactions in a dimer and in a solid.

The HF-SCCF method has been employed above to discuss structures of $H_2O_2(s)$, $C_2H_2(s)$ and $N_2(s)$, which represent molecular solids with large, small and very small lattice energies, respectively. The purpose was to investigate the kind of crystallographic information that can be extracted by employing the HF-SCCF approach in conjunction with experimental findings.

Good agreement with the interpretation of neutron diffraction data is obtained for the structure of solid H_2O_2, with respect to both the unit-cell dimensions and the intramolecular torsion angle. Agreement with the interpretation of neutron diffraction data is obtained also in the case of the hot-phase structure of solid C_2H_2, in that the apparent shortening of the intramolecular bond distances is proposed to result from the molecular librations. Precessional motion, which is a particular two-dimensional libration montion, is proposed in the present study. Any interpretation based on the calculated shallow potential-energy surface of α-$N_2(s)$ must be hazardous. Experimental difficulties in making the α phase are understood in terms of two counteracting crystal structures. Lattice energies in qualitative agreements with experiment are obtained in all three cases.

Continuing investigations of the usefulness of the HF-SCCF approach mainly follows two lines:

(*a*) addressing the structural properties in many different molecular solids by calculating the relevant potential-energy surfaces;

(*b*) method development to include statistical-mechanics principles to provide detailed structural interpretations of the calculated potential-energy surfaces, which is under way.

The results of such investigations would test the validity of the partitioning of the interactions in a molecular solid into intramolecular and intermolecular contributions for each particular solid.

References

ABRAHAMS, S. C., COLLIN, R. L. & LIPSCOMB, W. N. (1951). *Acta Cryst.* **4**, 15–20.

ALMLÖF, J., FAEGRI, K. JR, FEYEREISEN, M. & KORSELL, K. (1991). *DISCO. A Direct SCF and MP2 Code.* Univ. of Minnesota, USA.

AMBROSE, D. & TOWNSEND, R. (1964). **60**, 1025–1029.

ANDERSON, A., SUN, T. S. & DUNKERSLOOT, M. C. A. (1970). *Can. J. Phys.* **48**, 2265–2271.

AVOIRD, A. VAN DER, WORMER, P. E. S. & JANSEN, A. P. J. (1986). *J. Chem. Phys.* **84**, 1629–1635.

BERNS, R. M. & VAN DER AVOIRD, A. (1980). *J. Chem. Phys.* **72**, 6107–6116.

BOLZ, L. H., BOYD, M. E., MAUER, F. A. & PEISER, H. S. (1959). *Acta Cryst.* **12**, 247–248.

BRITH, M., RON, A. & SCHNEPP, O. (1969). *J. Chem. Phys.* **51**, 1318–1323.

BROOKEMAN, J. R. & SCOTT, T. A. (1972). *Acta Cryst.* **B28**, 983–984.

BUSING, W. R. & LEVY, H. A. (1958). Abstract of the American Crystallographic Association Annual Meeting, Milwaukee, Wisconsin, p. 38.

BUSING, W. R. & LEVY, H. A. (1959). *Chemistry Division Annual Progress Report*, p. 66. Report ORNL-2782. Oak Ridge National Laboratory, Tennessee, USA.

BUSING, W. R. & LEVY, H. A. (1965). *J. Chem. Phys.* **42**, 3054–3059.

CAHILL, J. E. & LEROI, G. E. (1969). *J. Chem. Phys.* **51**, 1324–1332.

DONOHUE, J. (1961). *Acta Cryst.* **14**, 1000–1001.

DOVESI, R., SAUNDERS, V. R. & ROETTI, C. (1992). *CRYSTAL92 Users Manual.* Gruppo di Chimica Teoretica, Univ. di Torino, Italy and SERC Daresbury Laboratory, Warrington England.

FAST, H. & WELLS, H. L. (1972). *J. Mol. Spectrosc.* **41**, 203–221.

GANNON, D. J. & MORRISON, J. A. (1973). *Can. J. Phys.* **51**, 1590–1592.

GIAUQUE, W. F. & CLAYTON, J. O. (1933). *J. Am. Chem. Soc.* **55**, 4875–4889.

GIGUÈRE, P. A. & SECCO, E. A. (1954). *Can. J. Chem.* **32**, 550–556.

Handbook of Chemistry and Physics (1988–89). Edited by R. C. WEAST, p. F166. Cleveland, Ohio: The Chemical Rubber Co.

HINCHLIFFE, A. (1987). *Ab Initio Determination of Molecular Properties.* London: Institute of Physics.

HIRSCHFELDER, J. O., CURTISS, C. F. & BIRD, R. B. (1954). *Molecular Theory of Gases and Liquids.* New York: Wiley.

HÖHRL, E. M. & MARTON, L. (1961). *Acta Cryst.* **14**, 11–19.

JORDAN, T. H., SMITH, A. W., STREIB, W. E. & LIPSCOMB, W. M. (1964). *J. Chem. Phys.* **41**, 756–759.

KELLEY, K. K. (1935). Bulletin 383. US Department of the Interior, Bureau of Mines.

KOPUT, J. (1986). *J. Mol. Spectrosc.* **115**, 438–441.

MCMULLAN, R. K., KVICK, Å. & POPELIER, P. (1992). *Acta Cryst.* **B48**, 726–731.

PANAS, I. (1992). *Chem. Phys. Lett.* **194**, 239–243.

PANAS, I. (1993*a*). *Chem. Phys. Lett.* **201**, 255–260.

PANAS, I. (1993*b*). *Chem. Phys. Lett.* **206**, 312–317.

PANAS, I. (1993*c*). *Theor. Chim. Acta.* In the press.

PAULING, L. (1930). *Phys. Rev.* **36**, 430–443.
RUHEMANN, M. (1932). *Z. Phys.* **76**, 368–375.
SCHUCH, A. F. & MILLS, R. L. (1970). *J. Chem. Phys.* **52**, 6000–6008.
ST. LOUIS, R. V. & SCHNEPP, O. (1969). *J. Chem. Phys.* **50**, 5177–5183.
STREIB, W. E., JORDAN, T. H. & LIPSCOMB, W. N. (1962). *J. Chem. Phys.* **37**, 2962–2965.
SZABO, A. & OSTLUND, N. S. (1982). *Modern Quantum Chemistry: Introduction to Advanced Electronic Structure Theory*, ch. 6. New York: Macmillan.
VEGARD, L. (1929). *Z. Phys.* **58**, 497–501.
VENABLES, J. A. (1970). *Philos. Mag.* **21**, 147–166.
VENABLES, J. A. & ENGLISH, C. A. (1974). *Acta Cryst.* **B30**, 929–935.
WACHTEL, E. J. (1972). *J. Chem. Phys.* **57**, 5620–5621.

Acta Cryst. (1993). A**49**, 889–893

Evaluation of Reflection Intensities for the Components of Multiple Laue Diffraction Spots. II. Using the Wavelength-Normalization Curve

BY J. W. CAMPBELL

SERC Daresbury Laboratory, Warrington, Cheshire WA4 4AD, England

AND Q. HAO

SERC Daresbury Laboratory, Warrington, Cheshire WA4 4AD, England, and Department of Chemistry, University of Liverpool, Liverpool L69 3BX, England

(*Received* 29 *January* 1993; *accepted* 6 *July* 1993)

Abstract

In a Laue diffraction pattern, 10–20% of the spots result from the exact superposition of two or more reflections that are 'harmonics', *e.g.* hkl, $2h,2k,2l$ *etc.* The use of only the 80–90% of the reflections measurable as singles may not always be sufficient and evaluation of the intensities of the components of the multiple spots is therefore important. A procedure for this deconvolution is given, based on the varying nature of the wavelength-normalization curve. A feasibility trial has been carried out using a single Laue diffraction image of tetragonal hen egg white lysozyme (HEWL) recorded on an image plate. This allowed the intensities of 103 reflections to be evaluated from multiple spots. For these reflections, their agreement with monochromatic diffractometer data gave an R factor of 0.157 for 96 common reflections. An earlier paper described another procedure based on direct methods, which addressed the same problem.

1. Introduction

With the advent of synchrotron radiation, there has been renewed interest in the use of Laue diffraction as a method for obtaining diffraction intensities (Campbell *et al.*, 1987; Helliwell *et al*, 1989; Smith Temple & Moffat, 1987; Smith Temple, 1989; Bartunik, Bartsch & Huang, 1992). Usually, 80–90% of the spots in a single Laue diffraction pattern correspond to single reflections, each with its values of hkl and associated d (plane spacing) and λ (Cruickshank, Helliwell & Moffat, 1987). These are described as singles. The remaining 10–20% of the spots are doubles, triples or higher multiples. If a crystal contains a plane of spacing d, then the spacings $d/2$, $d/3$, or in general d/j, may also occur, where j is any positive integer, Bragg's law is simultaneously satisfied by the sets of values (d, λ), $(d/2, \lambda/2)$, ..., $(d/j, \lambda/j)$, ... and the diffraction spots are exactly superposed. For these, measurement of the spot intensity does not therefore give the component reflection intensities directly. The reflections that cannot be straightforwardly measured as singles are not randomly distributed in reciprocal space; a high proportion of them are low-order reflections, axial reflections or reflections in special planes ($hk0$, hhl *etc.*). The absence of these reflections can be a serious drawback if the data are to be used for structure solution, for example using direct methods. Also, in, for example, larger-unit-cell protein crystals, the absence of low-order reflections has been shown to give electron-density maps that have poor connectivity and are particularly difficult to interpret (Duke, Hadfield, Walters, Wakatsuki, Bryan & Johnson, 1992). For reasons such as these, there has been renewed interest in methods to deconvolute reflection intensities from spots that are multiples. Helliwell *et al.* (1989) have described one procedure for this deconvolution that uses the intensities of spots on successive films in a film pack and the variation of film absorption with λ. With the increasing use of image plates or electronic detectors, it is desirable to develop methods that do not depend on recording the data on such multifilm packs. Hao, Campbell, Harding & Helliwell (1993) have described a use of direct methods to carry out such a deconvolution. This paper describes a method that makes use of the nature of the wavelength-

ISSN 0108-7673